Mon. Not. R. Astron. Soc. **000**, 1–9 (2005) Printed 14 March 2005 (MN LATEX style file v2.2)

What a Local Sample of Spectroscopic Binaries can tell us about the Field-Binary Population

James Fisher⋆, Klaus-Peter Schröder, Robert Connon Smith
Astronomy Centre, Department of Physics and Astronomy, University of Sussex, Falmer, Brighton, BN1 9QH, UK

March 2005: revised version of MN paper ME792

ABSTRACT

We study a sample of spectroscopic binaries (SBs) in the local solar neighbourhood ($d \leqslant 100$ pc and $M_{\rm V} \leqslant 4$) in an attempt to find the distributions of the period, P, the primary mass, m_1, and the mass ratio q $(= m_2/m_1)$, as well as the IMF of the local population of field binaries. The sample was collated using available SB data and the *Hipparcos* catalogue, the latter being used for distances and to refer numbers of objects to fractions of the local stellar population as a whole. We use the better-determined double-lined SBs (SB2s) to calibrate a Monte-Carlo approach to modelling the q distribution of the single-lined SBs (SB1s) from their mass functions, $f(m)$, and primary masses, m_1. The *total* q distribution is then found by adding the observed SB2 distribution to the Monte-Carlo SB1 distribution. While a complete sample is not possible, given the data available, we are able to address important questions of incompleteness and parameter-specific biases by comparing subsamples of SBs with different ranges in parameter space. Our results show a clear peak in the q distribution of field binaries near unity. This is dominated by the SB2s, but the flat distribution of the SB1s is inconsistent with their components being chosen independently at random from a steep IMF.

Key words: binaries: general – binaries: spectroscopic – stars: statistics.

1 INTRODUCTION

Much has been published on binary statistics and much of this has been concerned with the statistics of spectroscopic binaries (SBs) (e.g. Goldberg, Mazeh & Latham 2003; Halbwachs et al. 2003; Boffin, Cerf & Paulus 1993; Boffin, Paulus & Cerf 1992). Among the statistics discussed three of the most important have been the distributions of period (P), primary mass (m_1) and mass-ratio ($q = m_2/m_1$, where the primary in this paper is always taken to be the more massive star). These three parameters in particular are important as they present a set of variables that suffice to describe the principal properties of a binary system and its evolutionary path. Many papers have also been published specifically just on the mass-ratio distributions of SBs (e.g. Hogeveen 1991; Trimble 1974, 1978, 1987, 1990). The question of whether there is a peak in the q distribution near $q = 1$ has been a matter of debate for some time, on which we hope to shed some light in this paper. For instance the recent paper of Goldberg et al. (2003) found a distinct bimodal distribution; however, unlike ours, their sample was not confined to a particular volume and so might be expected to exhibit biases related to this fact.

The Initial Mass Function (IMF) of binaries is also of interest and, together with the period distribution, is important for the validation of star formation models. The IMF and P distributions are also important for understanding the chemical evolution of the Galaxy: interacting binary systems have more complex evolutionary pathways by which material can be lost to the Interstellar Medium (ISM) than single stars, leading, for example, to important systematic corrections to predictions of the carbon yield (Tout et al. 1999). Binary-system population synthesis models may then give a more complete idea of the enrichment of chemical elements in the ISM. This kind of modelling has been done before for single stars but to date studies of this kind for double stars have had to make certain assumptions about the P, m_1 and q distributions and the IMF.

There have also been studies of stars within galactic clusters (e.g. Kähler 1999) which are thus magnitude-limited and occupy specific limited volumes, as is the case for our sample, but which constitute very specific subsets of stars all of a particular age. Cluster stars are also in the process of diffusing from the cluster at a significant rate over time-scales of the order of 10^8 yrs. Hence the statistics of cluster binaries, while interesting in their own right, are not necessarily representative of binaries in general, or field binaries in particular and we do not consider them further.

What has not been done before to our knowledge is a study of the statistics of a distance and luminosity-limited sample of field binaries that is, as far as is possible with existing data, evolutionarily unbiased and complete.

⋆ E-mail: jfisher@sussex.ac.uk

In this paper we derive the distributions for the period P, primary mass m_1, mass ratio $q = m_2/m_1$ (m_2 being the mass of the secondary so that $q < 1$) and the IMF for a distance and luminosity-limited sample of SBs in the local solar neighbourhood $d \leqslant 100$ pc and $M_{\rm V} \leqslant 4$ and from there are able to make some deductions about these same distributions for the general population of field binaries. Because our sample is luminosity-limited, the only systems we will be missing completely will be those with primary mass $m_1 < 1.1\,{\rm M}_\odot$ on the Main Sequence. This luminosity cut-off makes the sample as unbiased as possible in an evolutionary sense.

While the sample is certainly *not* complete to the distance and luminosity limits stated, we believe that it is as complete as it is possible to make it without seriously compromising the sample size, and so without also compromising the conclusions drawn from the study. Although the sample is far from complete in absolute terms, we are able to make an assessment of the incompletenesses and are thus able to attempt to compensate for them. We thus believe that our sample is the best approximation to a volume-limited sample possible with the data currently available (to be truly volume-limited the sample would have to include *all* objects to the specified distance and luminosity limits).

2 THE SAMPLE

The spectroscopic binary data for the study was taken from the Eighth Catalogue of Orbital Elements of Spectroscopic Binary Systems (Batten, Fletcher & MacCarthy 1989), hereafter referred to in this paper as the 'Batten' catalogue, supplemented by other data of R.F. Griffin, both published (see the synopsis paper Griffin 2000 and others of that series) and unpublished (private communication), hereafter referred to as 'RFG' data. The Batten catalogue was until recently[1] the most comprehensive catalogue of SBs available, its selection criterion simply being to include all SB data available at the time of compilation. It thus encompasses a very diverse range of motivations for observation from all the many contributors, and so will contain a variety of selection effects, which are largely unknown apart from the tendency mentioned below to favour shorter-period systems. The inclusion of the RFG data was designed firstly to increase the size of the available dataset (many more objects having been observed since publication of the Batten catalogue in 1989, many of them by Roger Griffin), and secondly to attempt to compensate for the inevitable bias of the Batten catalogue towards shorter-period systems (inevitable because of the difficulties involved in sustaining consistent observing programmes for longer-period systems, as Roger Griffin has been able to do).

The Batten catalogue consists of 1469 SBs and the RFG data of 498 SBs. The combined Batten and RFG dataset (after removing duplicated objects) was filtered to a distance of 100 pc and limiting absolute magnitude of 4 ($d \leqslant 100$ pc and $M_{\rm V} \leqslant 4$) by correlating entries with the *Hipparcos* catalogue. The correlation was done by HD number, or by coordinates (corrected for precession) if no HD number existed, using the *Hipparcos* parallaxes and apparent magnitudes to calculate distances and absolute magnitudes. The cutoff for absolute magnitude was chosen in such a way that the sample should (to that magnitude) be as complete and homogeneous as possible, while at the same time having a sufficient number of systems to derive reasonable statistics. The chosen limiting absolute magnitude of 4.0 translates to an apparent magnitude of 7.5 at 50 pc and to 9.0 at 100 pc. The *Hipparcos* catalogue is complete to $m_{\rm V} = 7.3$, and in some areas down to $m_{\rm V} = 9.0$ (Perryman et al. 1997; Schröder & Pagel 2003), so all the SBs in our initial dataset of 1803 distinct stars that are closer than 50 pc (more precisely 46 pc) and brighter than $M_{\rm V} = 4$ should have been identified via the comparison with *Hipparcos*, and a reasonable fraction of those closer than 100 pc should also have been identified. A fainter limit would have created an inconsistent sample that, while having data from more systems at close distances, would be missing a lot of fainter systems at greater distances; it is already clear from the number in our final sample that many of the systems in the SB catalogues lie beyond 100 pc. The fainter limit would have led to a much steeper fall-off of completeness with distance than we find in our chosen sample, creating a sample that was harder to analyse. As mentioned above, because our sample is luminosity-limited with an absolute magnitude limit of ($M_{\rm V} \leqslant 4$), the only systems we will be missing completely will be those with primary mass $m_1 < 1.1\,{\rm M}_\odot$ on the Main Sequence.

When filtered in this way, the sample consists of 371 SBs: 145 double-lined SBs (SB2s) and 226 single-lined SBs (SB1s). It is this sample that we work with in the analysis that follows in the rest of the paper.

[1] The Ninth Catalogue has just appeared (Pourbaix et al. 2004).

Table 1. Period/evolutionary categories. The numbers of SBs are for $d \leqslant 100$ pc and $M_{\rm V} \leqslant 4$.

Category	Period range / days	SB1s	SB2s	Total SBs
(i)	$P \geqslant 500$	73	15	88
(ii)	$500 > P \geqslant 10$	84	60	144
(iii)	$10 > P \geqslant 1$	62	63	125
(iv)	$P < 1$	7	7	14
TOTALS		226	145	371

3 DISTRIBUTIONS

3.1 Period (P) distribution

The period distribution was found directly from the spectroscopic binary data. For later use in evolutionary studies the periods were divided into the four categories given in Table 1. It is intended that the four period categories should correspond roughly to the following four evolutionary scenarios:

(i) $P \geqslant 500$ d. Systems that will interact, if at all, at a late stage in their evolution, with the primary well on its way up the Asymptotic Giant Branch (AGB).

(ii) 500 d $> P \geqslant 10$ d. Systems that interact as the primary evolves onto the Red Giant Branch (RGB) or the AGB.

(iii) 10 d $> P \geqslant 1$ d. Systems that interact on the early RGB or as the primary leaves the Main-Sequence and enters the 'Hertzsprung Gap'.

(iv) $P < 1$ d. Systems that interact while on the late Main Sequence or earlier (contact systems).

To investigate the behaviour of the observed period distributions within different volumes *within* our 100 pc sample, the fractions of SBs (of all systems, single and multiple, determined from *Hipparcos*) in the above period categories were determined for volumes of radius 20 to 100 pc in steps of 2 pc for $M_{\rm V} \leqslant 4$. The absolute magnitude cutoff (the same as for the rest of the study) avoids the increasing incompleteness that would otherwise result

with increasing distance (without the cutoff we would include too many faint stars, many of which could reasonably be supposed to be unrecognised binaries). The results are shown in Fig. 1. The figure demonstrates well the quality of the data to 30 pc. For volumes much smaller than $d = 30$ pc the data are of little statistical significance due to the low absolute numbers involved (e.g. at 25 pc there are 12, 11, 8 and 0 systems in P categories (i) to (iv) respectively out of a total of 284 *Hipparcos* objects). The low numbers cause the fractions to vary somewhat erratically below 30 pc and so are also of little use in determining the trends. The results will be discussed in more detail in Section 4.

Clearly, a significant fraction of the systems are missing, but we can estimate the complete fractions for each category by extrapolation to 0 pc. Although the data are for SBs, the extrapolations will necessarily be the fractions of *all* binary/multiples (with respect to all stellar objects, single and multiple) as all binaries will be detectable as SBs at 0 pc. The extrapolation works because the further out in the sample we go, the less likely it is that a binary system is known as an SB. Therefore, as we go in the opposite direction, towards 0 pc, the fraction of systems that are detectable as SBs increases, and we get closer to the values of the unbiassed fractions. Fitting curves to the data from 100 pc to 30 pc, we were thus able to determine what the complete fractions *would* be at $d = 0$ pc.

Categories (i) and (ii) were fitted by cubic polynomials and category (iii) by a quadratic curve. The choice of curve was determined by its shape as well as the closeness of the fit: quadratics for categories (i) and (ii) and a cubic for category (iii) all gave curves that changed from convex to concave with distance and hence were not plausible. A cubic fit may be preferred on the grounds that it is what might be expected for number density within a spherical volume (the 100 pc limit is not large enough for the thickness of the galactic disc to become relevant (Schröder & Pagel 2003), in which case a quadratic fit might have been expected instead) but they are also more suseptible to errors in extrapolations due to the higher order term. The levelling out of the curves at larger distances is roughly what one would expect on the basis of the kind of bias expected at different distance regimes. At closer distances an apparent magnitude bias would be expected, as the brighter a system's $m_{\rm V}$ the more likely it would be to be known as an SB, while at larger distances one would expect a random selection bias due to the effectively random basis on which systems are chosen for study, causing the fraction of SBs to tend to a constant value at larger distances. For category (iv) it wasn't possible, or realistic, to do anything more with the data than to make a linear fit over the same distance range, this category being considerably limited in what we can do with it by its low absolute numbers.

The fits were made over as large a range of distances as possible before low absolute numbers made the data unreliable, in each case from 100 pc to 30 pc. Clearly it is difficult to estimate the errors on such extrapolations and the fractions are not necessarily going to be very accurate. However the fractions given by quadratic fits for categories (i) and (ii) instead of the cubic fits used can be used to give some idea of the errors involved. In both case the quadratic fits had lower constants, D, and hence lower fractions at 0 pc. Taking these differences into account the accuracy of the extrapolations is estimated to be of the order of 10%. Details for all four categories are given in Table 2. The extrapolations give the following estimates for the complete fractions of SBs in the four period categories (equal to the value of the constants D in Table 2): 0.140, 0.158, 0.0580 and 0.00154, giving a total binary fraction of 0.36 ± 0.11 (for stars brighter than $M_{\rm V} = 4$).

Table 2. Polynomial fits for Period categories: *Fraction* $= Ad^3 + Bd^2 + Cd + D$, where d is distance in pc. There are 36 data for each category (30 pc to 100 pc in steps of 2 pc). The constant D is also equal to the extrapolated fraction at 0 pc.

	A	B	C	D
(i)	$-1.05 \cdot 10^{-7}$	$3.33 \cdot 10^{-5}$	$-3.59 \cdot 10^{-3}$	0.140
(ii)	$-1.89 \cdot 10^{-7}$	$4.72 \cdot 10^{-5}$	$-4.28 \cdot 10^{-3}$	0.158
(iii)	0	$3.82 \cdot 10^{-6}$	$-8.40 \cdot 10^{-4}$	$5.80 \cdot 10^{-2}$
(iv)	0	0	0	$1.54 \cdot 10^{-3}$

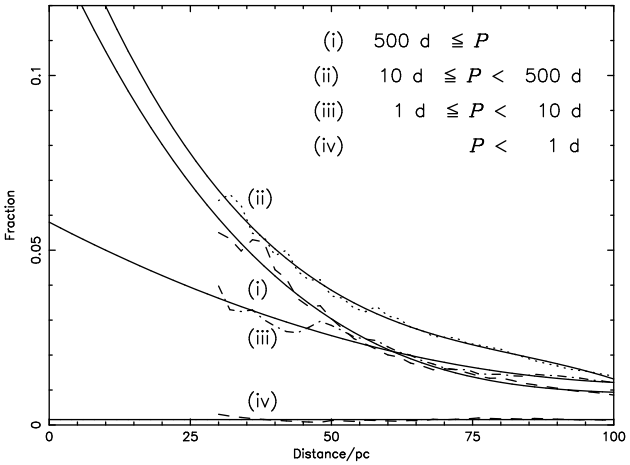

Figure 1. Period distributions of all SBs in the sample for the four period categories given in Table 1, together with extrapolations to 0 pc. Fractions to a particular distance are the fractions of *all* systems (single and multiple) with $M_{\rm V} \leqslant 4$ in the *Hipparcos* catalogue to that distance.

The above completes the more general analysis of the incompleteness of the sample. Selective incompletenesses will be considered in Section 4.

3.2 Primary-mass (m_1) distribution

Firstly, the *Hipparcos* parallaxes and apparent visual magnitudes of the systems, $m_{\rm V}$, were used to calculate the absolute visual magnitudes, $M_{\rm V}$. The primary masses of the SBs were then estimated from $M_{\rm V}$ by correcting for an average contribution of the secondary and applying a mass-luminosity relationship.

The absolute magnitude of the primaries, $M_{\rm V_1}$, were estimated using the following magnitude offsets from the absolute magnitude of the system, $M_{\rm V}$:

$$M_{\rm V_1} = M_{\rm V} + 0.50 \ \ (\text{for SB2s}) \quad (1)$$

$$M_{\rm V_1} = M_{\rm V} + 0.20 \ \ (\text{for SB1s}) \quad (2)$$

The offsets are necessary as the presence of even a visually unseen companion can make a significant difference to the magnitude of the system (see the discussion of ζ Aurigae systems below).

The offset for SB2s was determined by the clear peak of their q values (Section 3.3) near 1, with an average q of ≈ 0.84 (see Fig. 5 in that section). This means that the average SB2 secondary is about 40 per cent less luminous than the primary and so would contribute about 0.5 mag to the system's $M_{\rm V}$. (It should be noted in passing that the individual magnitudes of the SB primaries and secondaries are not usually known, even in the case of SB2s. Where the Batten

catalogue sometimes quotes two magnitudes these are in fact the maximum and minimum magnitudes of the system if the apparent magnitude of the system is variable.)

The offset for SB1s is a mean figure suggested by two considerations. Firstly, if the luminosity of the secondary were, on average, 30 per cent less than that of the primary (equivalent to a magnitude difference between the primary and the system of 0.3) then the contrast of the secondary's spectral lines would be enough for them to be visible, and the system would be observed as an SB2 rather than an SB1. Secondly, the depths of eclipse in ζ Aurigae systems (typically also catalogued as SBs, for example ζ Aurigae itself is in the Batten catalogue) are equivalent to the secondary contributing 0.1 - 0.2 mag. to the magnitude of the system. (See, for example, the photometry of the January 1989 eclipse of τ Persei given in Hall et al. 1991 and of the 1988 eclipse of 22 Vulpeculae in Griffin et al. 1993. It should also be noted that the only reason that ζ Aurigae and 22 Vulpeculae are known as SB2s is because their secondaries are visible in the ultraviolet band. For observations of ζ Aurigae systems in the visible waveband they are usually only seen as SB1s, as for example is 22 Vul which is given in the Batten catalogue as an SB1.) From these two considerations we therefore adopted an offset of 0.2 mag to account for an average SB1 secondary's contribution to the luminosity of the system.

Alternatively, we can argue from the q distribution that results from our calculations. From Fig. 5, we see that typically $q \simeq 0.5$, with a rather large uncertainty because of the flat distribution. Using the same argument as above for SB2s, this would lead to a contribution of about 0.13 to $M_{\rm V}$, which is (within the uncertainties) consistent with the 0.2 offset we have assumed. To test the effect of the offset, we have run the calculation below again with a zero offset, and the results are qualitatively similar (see Section 3.3).

A number of different mass-luminosity relationships were used to determine m_1 from $M_{\rm V_1}$ according to the evolutionary status of the primary. The evolutionary status was determined from its location on an HRD using the $B-V$ colour index from the *Hipparcos* catalogue and the value of $M_{\rm V_1}$ already calculated. The HRD was divided into a number of regions based on the characteristic regions used by Schröder (1998) and Schröder & Sedlmayr (2001) (see Fig. 2). For main sequence stars the mass-luminosity relationship used was for stars half-way through their H core-burning phase obtained from detailed theoretical stellar models computed with the well-tested evolution code of Peter Eggleton (Pols et al. 1998). The other mass-luminosity relationships are from Schröder & Sedlmayr (2001) and Schröder (1998). We thus have the following set of equations for m_1:

For Main Sequence primaries, both

$$B-V < (M_{\rm V_1}+1.50)/5.16 \quad (3)$$
$$\& \quad M_{\rm V_1} \geqslant -1.50 \quad (4)$$

and

$$B-V < 0 \quad (5)$$
$$\& \quad M_{\rm V_1} < -1.50 \quad (6)$$

use the following mass-luminosity relation

$$m_1 = (3.57 - 1.40M_{\rm V_1} + 0.311{M_{\rm V_1}}^2 - 0.027{M_{\rm V_1}}^3)\,{\rm M}_\odot \quad (7)$$

For Blue-loop giants:

$$B-V \geqslant (M_{\rm V_1}+1.50)/5.16 \quad (8)$$

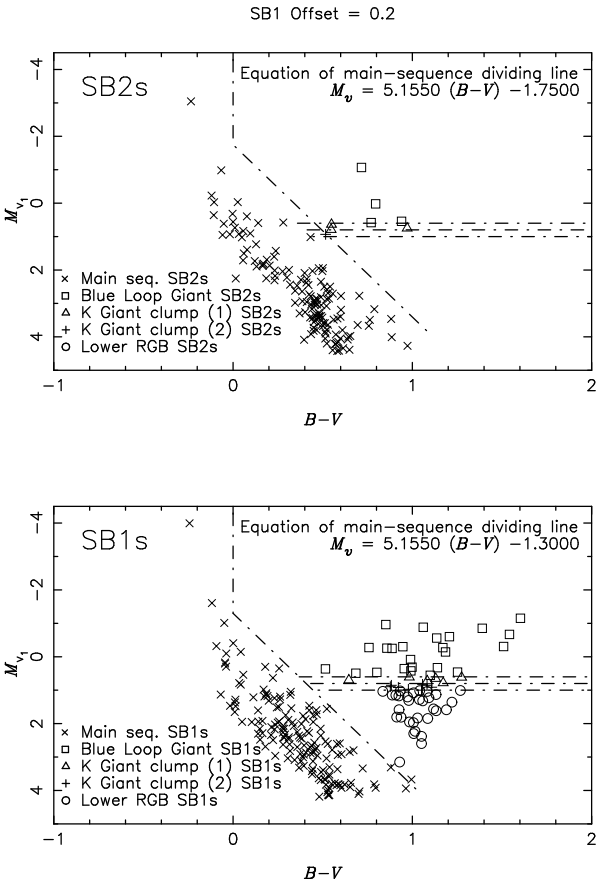

Figure 2. Evolutionary categories for SB2s and SB1s. These are used to determine which mass-luminosity relationship to use in estimating the masses of the primaries.

$$M_{\rm V_1} < 0.6 \quad (9)$$
$$m_1 = (-0.852M_{\rm V_1} + 2.81)\,{\rm M}_\odot \quad (10)$$

For K giant clump stars (subgroup 1):

$$B-V \geqslant (M_{\rm V_1}+1.50)/5.16 \quad (11)$$
$$0.6 \leqslant M_{\rm V_1} < 0.8 \quad (12)$$
$$m_1 = 1.8\,{\rm M}_\odot \quad (13)$$

For K giant clump stars (subgroup 2):

$$B-V \geqslant (M_{\rm V_1}+1.50)/5.16 \quad (14)$$
$$0.8 \leqslant M_{\rm V_1} < 1.0 \quad (15)$$
$$m_1 = (-0.852M_{\rm V_1} + 2.2)\,{\rm M}_\odot \quad (16)$$

For Lower RGB giants:

$$B-V \geqslant (M_{\rm V_1}+1.50)/5.16 \quad (17)$$
$$M_{\rm V_1} \geqslant 1.0 \quad (18)$$
$$m_1 = 1.25\,{\rm M}_\odot \quad (19)$$

The resulting distributions of estimated primary masses are shown in Fig. 3.

3.3 Mass-ratio ($q = m_2/m_1$) distribution

The q distribution for SB2s was found directly from the observed orbital semi-amplitudes, K_2 and K_1, the period, P, and the eccentricity, e, via:

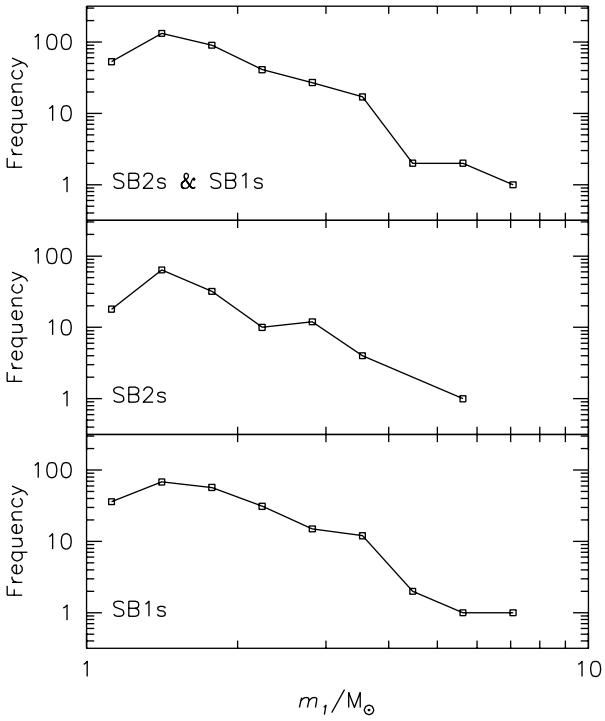

Figure 3. m_1 distributions determined in Section 3.2.

$$m_{1,2}\sin^3 i = 1.036\cdot 10^{-7}(1-e^2)^{3/2}(K_2+K_1)^2 K_{2,1} P \quad (20)$$

where $m_{1,2}$ have units of solar masses ($M_\odot$), $K_{1,2}$ have units of km s^{-1} and P has units of days (Hilditch 2001, p46). Hence:

$$q = \frac{m_2}{m_1} = \frac{m_2 \sin^3 i}{m_1 \sin^3 i} = \frac{K_1}{K_2}. \quad (21)$$

The q distribution for SB1s however is not so easy to determine. The closest one can get to q directly is the following function of the mass function, $f(m)$, and the primary mass, m_1:

$$\frac{f(m)}{m_1} = \frac{q^3 \sin^3 i}{(1+q)^2}. \quad (22)$$

The mass function is calculated from the observed period, P, primary orbital semi-amplitude, K_1, and eccentricity, e,

$$f(m) = 1.036\cdot 10^{-7}\,(1-e^2)^{3/2}\,{K_1}^3\,P \quad (23)$$

using the same units as for equation 20. The primary mass, m_1, may be determined as in Section 3.2.

There are a number of different methods for determining the underlying q distribution from the $f(m)/m_1$ distribution. Two of the most commonly used are:

(1) Richardson-Lucy iterative method (not used in this paper). This is a method that was first developed by Richardson (1972) for image restoration in optics and then first adapted for astronomical use by Lucy (1974) for the deconvolution of unknown distributions. It has since been used on a number of occasions for deconvolving q distributions from observed distributions (e.g. Hogeveen 1991). As it is not used in this paper no further details of this method shall be given here.

(2) Monte-Carlo simulation (used in this paper in a refined form). This involves calculating the $q^3\sin^3 i/(1+q)^2$ distributions from a variety of postulated q distributions and matching them to the observed $q^3\sin^3 i/(1+q)^2$ distribution.

[For other methods see, for instance, Halbwachs (1987).]

While the Monte-Carlo method might be considered to be somewhat unsophisticated, especially given some of the assumptions that have had to be made in the past to make the method work (see below), we have been able to introduce a number of constraints and tests that we hope improve it somewhat and make it more robust. By contrast, methods such as Richardson-Lucy are not as direct and are also more dependent on initial assumptions.

3.3.1 A short review of previous Monte-Carlo studies

This method has been used on many occasions before, but a number of restrictions and/or assumptions have always had to be made in order to make it work. For example Boffin et al. (1993) restricted the sample to 213 spectroscopic binaries with red giant primaries, assumed a constant mass for the primaries and also an average value of $\sin^3 i$. Trimble's study (Trimble 1990) was also limited to a subset of SBs, 164 in this case, most of which were K giants, their primary masses being determined from their spectral classes.

A major problem encountered in Monte-Carlo determinations of q distributions is how to take account of the unknown orbital inclination angle i. The effect of any assumed i distribution is made more critical by the dependence of $f(m)/m_1$ on $\sin^3 i$. Typically the unknown i s have been accommodated by assuming an average value for $\sin^3 i$. As well as being a bit crude, and so perhaps of better use where more rigorous methods may not be possible, this method does have other distinct problems. Boffin et al. (1993) show that, using this method, it is possible to obtain correct looking results for a decreasing q distribution while giving a totally wrong result for the case where $f(q)\propto 1/q$. In fact, for this reason Boffin et al. (1993) discard a simple Monte-Carlo approach despite others such as Trimble (1990) and Hogeveen (1991) finding that it gives results similar to more sophisticated approaches such as the Richardson-Lucy method. Mazeh & Goldberg (1992) also find that it produces erroneous results; in their paper they show two graphs of simulations with invented q distributions and demonstrate how badly they are reconstructed using this method: an even distribution is reconstructed as a decreasing distribution with constant gradient, and a distribution increasing towards $q=1$ is reconstructed as an upside-down U-shaped distribution. They then go on to show that these results are a consequence of some of the initial assumptions of the method being invalid. Another procedure is to adopt a 'model-fitting' approach where the probability of detecting a system with a certain inclination, i, is set by theoretical considerations. This however usually involves making somewhat *ad hoc* theoretical assumptions.

Trimble (1974, 1990) took two approaches to the unknown $\sin^3 i$ values: the direct approach using an average value of $\sin^3 i$, and a model-fitting approach that assumed the probability, p, of there being an orbit of inclination, i, to be proportional to a certain function: $p(i)\propto \sin i$ in Trimble (1990), as suggested in Halbwachs (1987), and $p(i)\propto \sin^2 i$ in Trimble (1974). However the average $\sin^3 i$ values were themselves determined by assuming that the probability of detecting a system was proportional to a particular function. Halbwachs (1987) used three methods: the average $\sin^3 i$ method, and two other methods not discussed here: one due

to Abt & Levy (1985) and the other due to Jaschek & Ferrer (1972). None of these methods is entirely satisfactory.

3.3.2 Refined Monte-Carlo Method (used in this paper)

In the present study we attempt to avoid some of the problems previously encountered with this method by introducing some of our own refinements, ones that are largely made possible by the use of the *Hipparcos* catalogue. For instance, the subset of better-known SB2s was used to derive constraints that could then be applied to all SBs. For the masses, we were able to go a step further than previous studies by using the *Hipparcos* parallaxes to determine absolute magnitudes, and from there obtain the primary masses directly from their evolutionary status determined from their position on an HRD (as discussed above in section 3.2). We thus circumvented the dual problems of having to make assumptions about the unknown masses and of being restricted to a limited sample of stars of a particular luminosity class. The study was hence opened up to stars of any evolutionary status, subject only to a limiting absolute magnitude of 4 as in the rest of our study.

We also used a method of random inclinations, i, to avoid having to assume an average value of $\sin^3 i$. The angle i varies between 0° and 180°, but in practice systems with inclinations near 0° or 180° will not be easily visible as the components of their radial velocity in our line of sight will be too small to measure reliably. Systems with i near to 0° or 180° will thus tend to be missed in surveys. For our Monte-Carlo procedure we have assumed therefore that i varies between a minimum cutoff angle α_0 and 90° (sufficient as i only appears as $\sin^3 i$ in the equations). The probability of detecting a system is therefore zero for i less than α_0 and proportional to $\sin i$ between α_0 and 90°, i.e. $p(i) = 0$ for $i < \alpha_0$ and $p(i) \propto \sin i$ for $\alpha_0 \leqslant i \leqslant 90^\circ$. The reason for the proportionality to $\sin i$ is that the projection of the SB's orbit onto the line of sight is proportional to $\sin i$, and hence so is the probability of observing the system as an SB. This means that a initial uniformly random variate, x, has to be transformed to $i = \arccos(1 - x)$ (the mathematical reasoning behind the transformation is given in section 7.2 of Press et al. 1993). This is, we think, more reasonable than previous assumptions that have been made (and indeed have had to be made).

A problem with the estimated mass procedure as implemented is that the masses for the main sequence primaries (that is, the greater proportion of them) are taken from half-way through their H core-burning phase. In reality the masses will be 'smudged out' to either side of these values. To simulate this when calculating the $f(m)/m_1$ distribution from random inclinations a 'Smudge Factor', ζ, was therefore introduced so that the simulated $f(m)/m_1$ values are multiplied by a random factor of up to $(1 \pm \zeta)$.

The values of α_0 and ζ were found by comparing the $f(m)/m_1$ distribution for SB2s from two different sources: (i) from their q values and random i values, $\alpha_0 \leqslant i \leqslant 90^\circ$ for different values of α_0 and ζ (1000 random i values per q value) and (ii) from their mass functions, $f(m)$, and estimated primary masses, m_1. The $f(m)/m_1$ distributions were plotted as histograms, 5 bins per 0.1 on the $f(m)/m_1$ axis (see Fig. 4 for an example of the histograms from each source for the α_0 calibration).

The main effect of the smudging out of the masses on the $f(m)/m_1$ distribution from (ii) was that the maximum value of $f(m)/m_1$ became greater than the maximum theoretical value of 0.25. (A smaller additional effect was that the slope of the distribution towards the maximum $f(m)/m_1$ value was slightly shallower than that from (i).) From a range of values of ζ from 0.0 to 0.5 in steps of 0.1, $\zeta = 0.20 \pm 0.05$ was selected as giving the same maximum value of $q^3 \sin^3 i/(1 + q^2) = f(m)/m_1$, from (i) as from (ii).

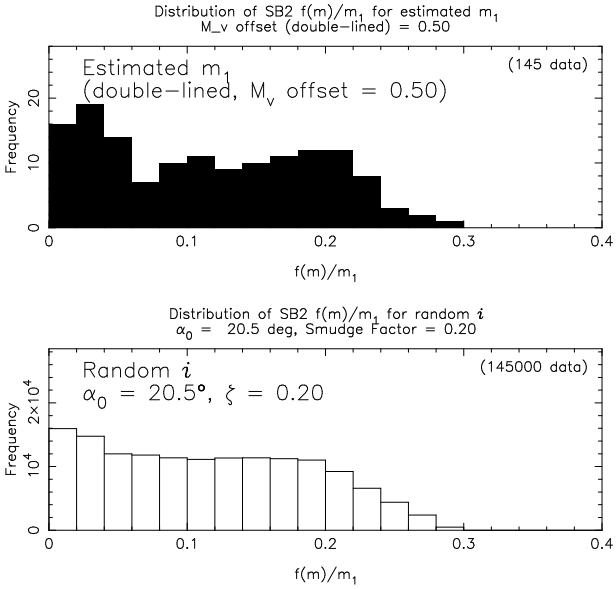

Figure 4. Examples of histograms for the α_0 calibration taken from the two sources given in Section 3.3.2. The ζ calibration has already been performed so that the maximum values of $f(m)/m_1$ are the same from both sources.

Once ζ had been determined in this way the value of α_0 could then be found by comparing the ratios of the first bin ($f(m)/m_1$ from 0 to 0.025) to the total frequency. By this means the best match was found to be for $\alpha_0 = 20.5 \pm 1.0^\circ$.

The determination of α_0 and ζ were both cases demonstrating how the better known SB2s could be used to calibrate parameters for the Monte-Carlo approach to the SB1s. Not only were we able to validate methods before using them for the unknown SB1 q distribution but we were able to determine fine-tuning parameters for the simulation as a whole. We did then have to assume that the values of α_0 and ζ were the same for SB1s as for SB2s. This would be reasonable if the SB2s and SB1s have similar selection criteria and if the probabilities of detecting a spectroscopic binary as an SB2 or an SB1 are independent. The similar behaviour of the fractions of SB2s and SB1s in Fig. 7 in Section 4 gives us some confidence that this is indeed the case.

To perform the Monte-Carlo simulation a variety of plausible q distributions were constructed by dividing the range of q values from 0 to 1 into ten equal bins and choosing frequencies for each bin. The resultant $f(m)/m_1$ distributions were then calculated for random values of the inclination, i, from α_0 to 90°, $p(i) \propto \sin i$, with random values of the smudge factor between $1 - \zeta$ and $1 + \zeta$. For each data point on the q distribution a thousand random values of i were used to make the resultant $f(m)/m_1$ distribution as smooth as possible. The total frequencies for the constructed $f(m)/m_1$ distributions ranged from 2×10^4 to 2×10^5. The $f(m)/m_1$ distribution was divided in each case into 25 bins from 0 to 0.25 (the maximum value of $f(m)/m_1$ for $q \leqslant 1$ being 0.25). We then had to assume, albeit from reasonable arguments, the offset to add to $M_{\rm V}$ to determine $M_{\rm V_1}$ for the SB1s (see equation 2 and the text afterwards).

The q distributions tried were systematic variations on the following 'types': exponential-like functions increasing in frequency towards $q = 1$ but with the rise starting at varying q values, 'hump-

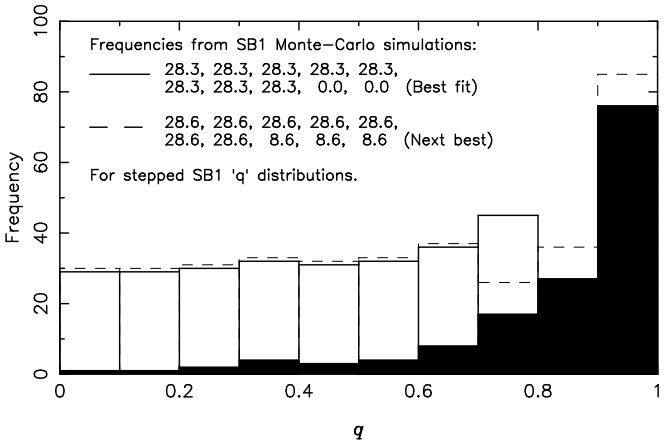

Figure 5. Histogram of the q distribution for SB2s and SB1s combined, SB2s on the bottom (filled-in) and SB1s on top (unfilled), for Monte-Carlo simulations of *stepped* SB1 q distributions. The solid line of the SB1s is the best fit, the broken line is the next best fit.

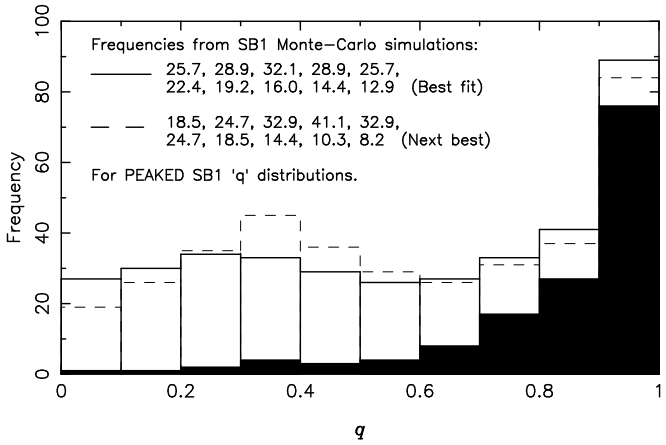

Figure 6. Histogram of q distribution for SB2s and SB1s combined for Monte-Carlo simulations of *peaked* SB1 q distributions. SB2s are on the bottom (filled-in) and SB1s on top (unfilled). The solid line of the SB1s is the best fit, the broken line is the next best fit.

functions' with a pronounced maximum at varying q values and different levels upon either side, and 'step-functions' with the step at varying q values and of varying size. As the resultant $f(m)/m_1$ distributions proved to be rather insensitive to many of the variations tried we settled on a step function as being a minimal solution requiring the fewest arbitrary assumptions.

However, given that other authors have found a preference for a bimodal distribution of q, with a secondary peak at around $q = 0.2$ (e.g. Staniucha 1979), we also present results from peaked q distributions to see whether the resulting $f(m)/m_1$ distributions match observations better or worse than the simple step function.

The test used to determine the optimal q distribution was to compare two ratios: the ratio of the frequency of the first bin ($0 < f(m)/m_1 \leqslant 0.01$) to the second ($0.01 < f(m)/m_1 \leqslant 0.02$) and the ratio of the frequency of the first bin to the total for the 5th to 25th bins ($0.04 < f(m)/m_1 \leqslant 0.25$). The first gives a measure of the rise in frequency at the low end of the distribution while the second ratio summarises the relationship of the size of the peak (invariably near $f(m)/m_1 = 0$) to the rest of the distribution. The observed ratios for the SB1 $f(m)/m_1$ distribution were 3.250 and 1.492 respectively. The best fit to these ratios for the q distributions tried was for a q distribution consisting of a level portion at a value of 20 for $0 < q \leqslant 0.8$ followed by a step down to zero and then continuing at zero for $0.8 < q \leqslant 1$. When normalised to the total number of observed SB1s this gave frequencies of 28.3, 28.3, 28.3, 28.3, 28.3, 28.3, 28.3, 28.3, 0 and 0 for the ten equally spaced bins from $q = 0$ to 1.

The Monte Carlo SB1 distribution is normalised to the total number of SB1s observed in our sample, to make it directly comparable with the observed SB2 distribution. If we then simply add the normalised SB1 and observed SB2 distributions with equal weight to produce an overall distribution we are assuming that there is no obvious bias in our sample towards observing SB2s. Looking at the statistics of SB2s and SB1s in the Batten catalogue and in the data from Griffin, there is if anything a bias towards SB1s: our final sample contains 61% SB1s and 39% SB2s. This lack of bias can probably be explained by the fact that most of the data requires long-term observing programmes that have only been possible where telescopes have been dedicated to the programme and the choice of which stars to observe has not been limited by the exigencies of time allocation committees. Target lists are compiled on the basis of detected variability, usually long before it is known whether the target is an SB1 or an SB2, and objects are kept on the target list until an orbit has been determined. This is certainly true for the Griffin data and seems likely to be true for the Batten catalogue as well, most of which dates from the era of long-term programmes at national or private university telescopes.

Table 3. A table of the two different sources used in the paper for the histograms of combined SB2 and SB1 q distributions. Given are the (normalised) frequencies for the 10 bins, q =0 to 1, and a comparison of the main features of the distributions.

Source	**Combined q distribution**	**General features**
Observed SB2 + stepped SB1 Monte-Carlo	29, 29, 30, 32, 31, 32, 36, 45, 27, 76	Peak, $q = 0.9$–1.0, Plateau, $q = 0$–0.6, at 0.4 of max.
Observed SB2 + peaked SB1 Monte-Carlo	27, 30, 34, 33, 29, 26, 27, 33, 41, 89	Main peak, $q = 0.9$–1.0, Broad peak, $q = 0.2$–0.4, at 0.38 of max.

Adding the Monte-Carlo SB1 q distribution to the observed SB2 distribution according to this equal weight prescription gives the combined SB q distribution shown for the step function in Fig. 5. This figure also shows the effect of adding the next best-fitting SB1 q distribution, the difference being slight as far as the overall shape of the total distribution is concerned. The figure clearly shows a peak towards $q = 1$. Furthermore, the peak comes primarily from the SB2 contribution, derived directly from the observed data, and so is unaffected by uncertainties in the SB1 distribution. Nonetheless, the q distribution is qualitatively similar if a zero offset is used in equation 2 instead of 0.2; quantitatively, the first four SB1 bins in the best fit with zero offset have frequencies of 32.3 instead of 28.3, and all the remaining bins have frequencies of 16.1. This has the effect, if anything, of accentuating the $q = 1$ peak in the overall distribution. Curiously, the zero offset case (which corresponds to the fainter component of the SB1 making no significant contribution to the total luminosity) puts some stars into the $q = 0.9 - 1$ bin. These systems presumably have evolved primaries that are much brighter than their unevolved companions.

The distribution with zero offset gives a hint of a second peak

for low q, so it is worth looking at the best-fitting q distributions with a peak. These are shown in Fig.6. However, the fit to the observed $f(m)/m_1$ distribution is much less good than for our preferred stepped q distribution, the peak for the best fit peaked distribution is not very pronounced (the best fit histogram is not very different from the one for a stepped distribution in Fig.5), and the peak at $q = 1$ is still dominant.

It is also interesting to compare our best-fitting q distribution with the one that would be predicted if we took the components at random from a steep IMF. This prediction has been made by Tout (1991), who considered an IMF steep above $1\,M_\odot$ but flat for smaller masses. For the SB2 distribution, he took the lower mass cut-off for both components to be $1\,M_\odot$ and found a curve that rose steeply from $q = 0$ to $q = 1$, similar to our SB2 distribution, although not so concentrated around $q = 1$. For the SB1 distribution he took the same lower mass cut-off for the primary but chose $0.2\,M_\odot$ as the cut-off for the secondary. This gave a q distribution with a strong peak at $q = 0.2$ and a curve that dropped smoothly to a low value at $q = 1$ (see Figure 6 of Tout 1991). The joint distribution is thus bimodal, similar to the result found by Staniucha (1979) illustrated in Figure 1 of Tout (1991). This strongly double-peaked distribution is not consistent with our q distribution, which is very flat for $q < 0.7$, even for the peaked distribution that we tried (Figs 5 and 6). We conclude that the components in our sample of binaries were *not* chosen independently and at random from the steep IMF that they seem to obey (see discussion in the next section). A similar conclusion was reached by Eggleton, Fitchett & Tout (1989) for a more restricted sample of visual binaries with two bright components.

Fig.7 demonstrates that the fractions of SB2s and SB1s of all stars (all entries in HIPPARCOS within 100 pc and the same absolute magnitude limit) behave rather similarly for varying limiting absolute magnitudes (the deviation at brighter M_V for SB2s being due to low absolute numbers). This to some degree justifies our using parameters derived from SB2s, such as the value of α_0, for SB1s as well. Note that here, as in the next section, we are dealing with M_V, and not M_{V_1}, as it is the selection biases on the *systems* that we are interested in.

Given that the SB2s and SB1s seem to have essentially the same selection criteria, the two distributions will also be independent of each other, the probability of detecting one set of lines or two then depending only upon the detector resolution. In this case, detecting one set of lines will be independent of detecting the other and it is thus justifiable to add the two q distributions together in the way we have done to produce Fig. 5.

4 DISCUSSION

So far, we have derived the observed period, primary mass and mass-ratio distributions for our distance-limited sample. If there are any serious selection effects, however, the true distributions could well be significantly different. Selection effects acting on the q distribution have already been discussed in detail in Section 3.3 and thus we can be confident of the reality of the peak in the q distribution near $q = 1$.

There is however another obvious selection effect possibly acting on the m_1 distribution that has not yet been considered: the possibility of a lower detection rate for less luminous binaries. This would be reflected in a less pronounced increase in the observed m_1 distribution towards smaller masses compared to the true present-day mass function (PDMF). In the *observed* distribution in Fig. 8,

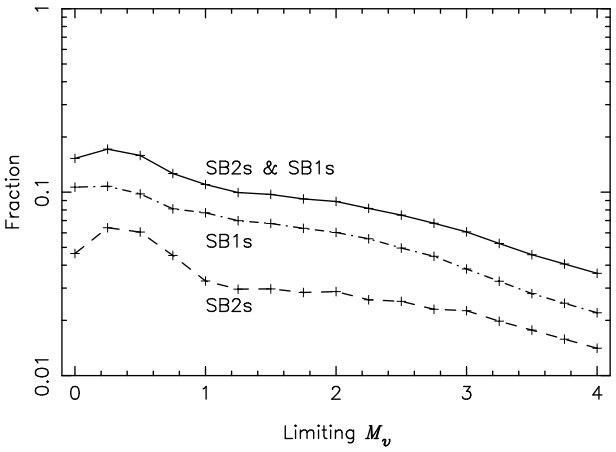

Figure 7. Fraction of SBs, distance $\leqslant$ 100 pc, for different limiting M_V. Fractions are defined as in Fig. 1.

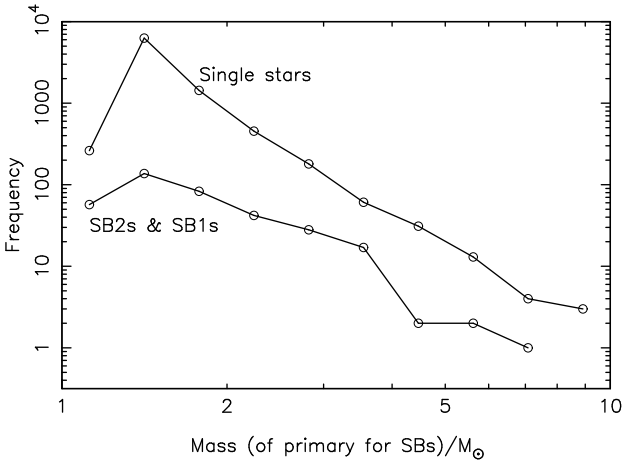

Figure 8. Frequency distribution of masses (in solar masses) of SB primaries and of single stars.

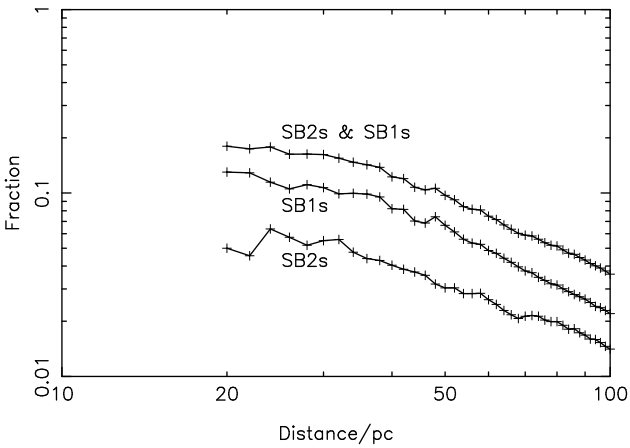

Figure 9. Fraction of SBs, $M_V \leqslant 4$, for different volumes up to 100 pc. Fractions are defined as in Fig. 1.

Table 4. Comparing the change in fraction with limiting M_V (Fig. 7) with the change with distance (Fig. 9).

Fig. 7: change of fraction with M_V.	**Fig. 9:** change of fraction with volume (max. distance of sample).
Decreasing average m_V & decreasing average mass going from left to right.	Decreasing average m_V but ***same*** average mass going from left to right.
Fraction falls by a factor of ~ 4.3 from M_V = 1 to 4.	Fraction falls by a factor of ~ 5 from 25 to 100 pc.
Could be due to a shallower PDMF and/or a selection effect.	Could ***only*** be due to an increasing incompleteness with increasing vol. & decreasing m_V.

Factor is approximately the same, therefore the decrease with M_V (and hence PDMF) is due to a selection effect. Therefore the PDMF of SB primaries is the same as that of single field stars.

$dN/d\log m_1 \propto m_1^{-2.8}$, while for single stars it is approximately $\propto m^{-4.8}$ (Schröder 1998). However, we need to know if this difference is genuine or due to a selection effect (or possibly both). To do this we look at the variation in detected SB fraction with volume (Fig. 9) and compare it with the variation with limiting M_V within 100 pc (Fig. 7).

Table 4 summarizes the following argument. The variation with M_V shows fractions with decreasing average mass and decreasing average *apparent* brightness as the absolute magnitude limit becomes fainter, while the variation with volume shows fractions which again have decreasing apparent brightness as the volume is increased but now have the *same* average mass for all volumes. The variation with volume shows a decrease in fraction by a factor of ~ 5 from 25 to 100 pc, while the variation with limiting M_V shows a decrease by a factor of ~ 4.3 over a corresponding range of $M_V = 1$ to 4 (a factor of 4 in distance being equivalent to a difference of 3 in magnitude). The decrease with limiting M_V could again be due to a shallower PDMF or a selection effect, but the decrease with volume could only be due to the increasing incompleteness as the volume enlarges (and apparent brightness decreases). The fact that the two fractions fall off by approximately the same factor shows that the decrease with M_V, and hence the shallower PDMF, is indeed due to a selection effect. The true PDMF and IMF of the binary primaries are therefore nearly identical to those of single field stars in the solar neighbourhood (Schröder & Pagel 2003 and references contained therein).

ACKNOWLEDGMENTS

We wish to express our special gratitude to R.F. Griffin for the generous use of his unpublished SB data which constitutes a significant fraction of the total sample studied. We also thank the *Centre de Données astronomiques de Strasbourg* (CDS) for their excellent internet database through which access was gained to the *Hipparcos* and Batten catalogues, and also the referee, Chris Tout, and colleagues at the Astronomy Centre at the University of Sussex, who gave much valuable advice on improving the paper. JF wishes to acknowledge the support of a Postgraduate Assistantship from the University of Sussex.

REFERENCES

Abt H.A., Levy S.G., 1985, ApJS, 59, 229
Batten A.H., Fletcher J.M., MacCarthy D.G., 1989, Publications of the Dominion Astrophysical Observatory, Vol. 17
Boffin H.M.J., Paulus G., Cerf N., 1992, in Duquennoy A., Mayor M., eds, Binaries as Tracers of Stellar Formation, Cambridge Univ. Press, Cambridge, England, p.26
Boffin H.M.J., Cerf N., Paulus G., 1993, A&A, 271, 125
Eggleton P.P., Fitchett M.J., Tout C.A., 1989, ApJ, 347, 998
Goldberg D., Mazeh T.& Latham D.W., 2003, ApJ, 591, 397
Griffin R.E.M., Hünsch M., Marshall K.P., Griffin R.F., Schröder K.-P., 1993, A&A, 274, 225
Griffin R.F., 2000, The Observatory, 120, 195
Halbwachs J.L., 1987, A&A, 183, 234
Halbwachs J.L., Mayor M., Udry S., Arenou F., 2003, A&A, 397, 159
Hall, Douglas S. et al., 1991, AJ, 101, 1821
Hogeveen S.J., 1991, PhD thesis, Univ. Amsterdam
Hilditch, R.W., 2001, An Introduction to Close Binary Stars. Cambridge Umiversity Press, Cambridge.
Jaschek C., Ferrer O., 1972, PASP, 84, 292
Kähler H., 1999, A&A, 346, 67
Lucy L.B., 1974, AJ, 79, 745
Mazeh T. & Goldberg D. 1992, ApJ, 394, 592
Perryman M.A.C. et al., 1997, A&A, 323, L49
Pols O.R., Schröder K.-P., Hurley J.R., Tout C.A., Eggleton P.P., 1998, MNRAS, 298, 525
Pourbaix D., Tokovinin A.A., Batten A.H., Fekel F.C., Hartkopf W.I., Levato H., Morrell N.I., Torres G., Udry S., 2004, A&A, 424, 727
Press W.H., Teukolsky S.A., Vetterling W.T. & Flannery B.P., 1993, Numerical Recipes in C, Cambridge University Press, Cambridge.
Richardson, W.H., 1972, Journal of the Optical Society of America, 62, 55
Schröder K.-P., 1998, A&A, 334, 901
Schröder K.-P., Pagel B.E.J., 2003, MNRAS, 343, 1231
Schröder K.-P., Sedlmayr E., 2001, A&A, 366, 913
Staniucha M., 1979, Acta astr., 29, 587
Tout C.A., 1991, MNRAS, 250, 701
Tout C.A., Karakas A.I., Lattanzio J.C., Hurley J.R., Pols O.R., 1999, in Le Bertre T., Lebre A., Waelkens C., eds, Proc. IAU Symp. 191, Asymptotic Giant Branch Stars, Astron. Soc. Pac., San Francisco, p. 447
Trimble V., 1974, AJ, 79, 967
Trimble V., 1978, The Observatory, 98, 163
Trimble V., 1987, Astron. Nachr., 308, 343
Trimble V., 1990, MNRAS, 242, 79